Translational Oncology
www.transonc.com
Volume 9 Number 1 February 2016 pp. 41–45 41

Monitoring Prostate Tumor Growth in an Orthotopic Mouse Model Using Three-Dimensional Ultrasound Imaging Technique[1,2]

Jie Ni[*,†], Paul Cozzi[†,‡], Tzong-Tyng Hung[§], Jingli Hao[*,†], Peter Graham[*,†] and Yong Li[*,†]

*Cancer Care Centre, St George Hospital, Kogarah, NSW 2217, Australia; [†]St George and Sutherland Clinical School, the University of New South Wales (UNSW), Kensington, NSW 2052, Australia; [‡]Department of Surgery, St George Hospital, Kogarah, NSW 2217, Australia; [§]Biological Resource Imaging Laboratory, the University of New South Wales (UNSW), Kensington, NSW 2052, Australia

Abstract

Prostate cancer (CaP) is the most commonly diagnosed and the second leading cause of death from cancer in males in USA. Prostate orthotopic mouse model has been widely used to study human CaP in preclinical settings. Measurement of changes in tumor size obtained from noninvasive diagnostic images is a standard method for monitoring responses to anticancer modalities. This article reports for the first time the usage of a three-dimensional (3D) ultrasound system equipped with photoacoustic (PA) imaging in monitoring longitudinal prostate tumor growth in a PC-3 orthotopic NODSCID mouse model ($n = 8$). Two-dimensional and 3D modes of ultrasound show great ability in accurately depicting the size and shape of prostate tumors. PA function on two-dimensional and 3D images showed average oxygen saturation and average hemoglobin concentration of the tumor. Results showed a good fit in representative exponential tumor growth curves ($n = 3$; $r^2 = 0.948$, 0.955, and 0.953, respectively) and a good correlation of tumor volume measurements performed *in vivo* with autopsy ($n = 8$, $r = 0.95$, $P < .001$). The application of 3D ultrasound imaging proved to be a useful imaging modality in monitoring tumor growth in an orthotopic mouse model, with advantages such as high contrast, uncomplicated protocols, economical equipment, and nonharmfulness to animals. PA mode also enabled display of blood oxygenation surrounding the tumor and tumor vasculature and angiogenesis, making 3D ultrasound imaging an ideal tool for preclinical cancer research.

Translational Oncology (2016) 9, 41–45

Introduction

Prostate cancer (CaP) is the most commonly diagnosed and the second leading cause of death from cancer in males in USA in 2014 [1]. Because CaP does not occur naturally in small rodents, mouse models are often established by subcutaneous and orthotopic injection of human CaP cells into immune-compromised mice. Mouse models play very important roles in CaP research. In preclinical oncology research, measurements of changes in tumor size obtained from diagnostic images are a standard method for monitoring responses to anticancer therapies [2]. For the orthotopic model which is broadly used in CaP research, it is very difficult to palpate the tumors and measure tumor growth, largely limiting the application of this model.

The recent development of noninvasive high-resolution imaging technologies for use with small laboratory animals has made equivalent measurements possible in mouse cancer models [3]. Ultrasound is a nonionizing and noninvasive imaging technique and provides good soft-tissue contrast and high spatial resolution without the need for administration of contrast agents, which makes itself an ideal tool for CaP imaging. Ultrasound is a quick, inexpensive, and

Address all correspondence to: Yong Li MD, PhD, Level 2, Research and Education Centre, St George Hospital, 4-10 South St, Kogarah, NSW 2217, Australia.
E-mail: y.li@unsw.edu.au

[1] This study was supported by NHMRC Career Development Fellowship, Surgical & Urological Research Foundation, Cancer Research Trust Fund at Cancer Care Centre, and Prostate and Breast Cancer Foundation.
[2] Conflicts of Interest: No potential conflicts of interest are disclosed.
Received 28 August 2015; Accepted 10 November 2015

1936-5233/16
http://dx.doi.org/10.1016/j.tranon.2015.11.011

portable procedure, and images of up to 40 μm in resolution can be obtained within 5 mm of the detector [4]. Despite the noninvasive and practical property of ultrasound, one of the major limitations of conventional ultrasound images is their inherently two-dimensional (2D) character because human anatomy is three-dimensional (3D). Thus, the specificity and accuracy of conventional 2D ultrasound are not satisfactory, being an arduous and time-consuming process prone to operator variability. 3D ultrasound imaging could significantly improve the accuracy and efficacy of tumor volume measurements obtained. Moreover, the recent development of photoacoustic (PA) imaging of tissues has demonstrated the ability to resolve common chromophores with spatial resolution exceeding that of ultrasound [5]. PA images relied on the endogenous contrast offered by blood and were presented as either a map of hemoglobin concentration or oxygen saturation (sO_2) based on the approximations [6]. Consequently, it enables imaging of vascular structures [5], blood oxygenation [7], and tumor angiogenesis [8].

In this study, we established the CaP orthotopic animal model using NODSCID mice, followed by longitudinal imaging studies which for the first time showed the feasibility and sensitivity of 3D ultrasound for monitoring prostate tumor growth in mice, and illustrate the use of PA ultrasound imaging to detect the tumor microenvironment of CaP in NODSCID mice.

Material and Methods

Cell Line and Cell Culture

PC-3 CaP cell line was cultured in RPMI-1640 supplemented with 10% (vol/vol) heat-inactivated fetal bovine serum (FBS), 50 U/ml of penicillin, and 50 U/ml of streptomycin. Cells were maintained in a humidified incubator at 37°C and 5% CO_2. All cell culture reagents were supplied by Invitrogen Australia Pty Ltd (Melbourne, VIC, Australia) unless otherwise stated. The identity of PC-3 was confirmed by short tandem repeat profiling and was tested within a few passages of initial authentication. The cell line was regularly tested to confirm the absence of mycoplasma contamination using the LookOut mycoplasma PCR detection kit (Sigma-Aldrich Pty Ltd, NSW, Australia).

Establishment of Orthotopic Xenograft Animal Model

Eight male, 6-week-old NODSCID mice (Animal Resources Centre, WA, Australia) were housed under specific pathogen-free conditions in facilities approved by the University of New South Wales Animal Care and Ethics Committee (ACEC Ethics No. 14/46A). Mice were kept at least 1 week before experimental manipulation. All mice remained healthy and active during the experiment. As described previously [9], mice were anesthetized with 2% isoflurane in oxygen, and 1×10^6 PC-3 CaP cells suspended in 50 μl of Dulbecco's phosphate-buffered saline (DPBS) were injected into the ventral prostatic lobe after exposure through a lower midline laparotomy incision. After the cell inoculation, prostate and other organs were returned to the body cavity, and incision was closed with sutures and metal clips. Starting from the first week after cell inoculation when the incision achieved a satisfactory healing and metal clips were removed, tumor progression was monitored weekly by ultrasound.

Ultrasonic Imaging Acquisition and Analysis

Mice were anesthetized with 1.5% to 2% isoflurane in oxygen and restrained on a heated stage during imaging. Prewarmed ultrasound coupling gel (Aquasonic 100, Parker Laboratories, Inc., Fairfield, NJ) was applied to the depilated skin before the imaging. Ultrasound imaging scan was performed using VisualSonics Vevo 2100 Ultrasound (VisualSonics Inc., Ontario, Canada). 2D images of mouse prostate and neighbor anatomies were acquired using a linear-array transducer (MS-400) in B-mode with 30-MHz center frequency that produces a 15-mm*15-mm field of view at the 12-mm focal depth. In the 3D acquisition method, the probe was attached to a 3D scanning motor that linearly drove the ultrasound probe across the mouse's skin as 2D images are acquired at regular spatial intervals so they are parallel and uniformly spaced at 100-μm intervals over a length of up to 14 mm. The predefined parallel geometry of the 3D images facilitates 3D image reconstruction. A full 2D and 3D image acquisition session requires less than 3 minutes.

PA imaging was performed using VisualSonics Vevo LAZR PA Imaging System (VisualSonics Inc., Ontario, Canada). The MS-400 transducer was integrated into a special housing that allowed both the ultrasound micro-coaxial cable and optical fiber bundles to be incorporated into the same package. An initial 3D survey of the tumor was performed in B-mode. A region of interest (ROI) was drawn around the tumors, and average values of sO_2 were calculated within instrument-specified ROI. Data were collected in 3D by scanning the transducer with the 3D motor while capturing 2D PA images.

Tumor Volume and Growth Curve Measurements

The 3D ultrasound images were processed and analyzed for calculation of tumor volume using Vevo Lab 1.7.0 software (VisualSonics Inc., Ontario, Canada). The reconstructed 3D image is displayed in a dynamic cube view format as a polyhedron with the appropriate image displayed on each face. The tumor boundaries were manually delineated in parallel slices in the 3D serials. The areas of the outlined contours were summed and multiplied by the interslice distance to compute tumor volume. Exponential volume growth curves were fit by linear regression; coefficients of determination were computed to assess the goodness of fit of the exponential function using a GraphPad Prism 6 package (GraphPad, La Jolla, CA). Upon mouse sacrifice at the end of experiments, primary prostate tumors were harvested and measured by a caliper. The gross tumor volumes were calculated as follows: length × width × height × 0.52 (in millimeters) [10]. Agreement of the gross pathology and ultrasound volume measurements was assessed using the graphical method of Bland and Altman [11].

Results

Ultrasound As a Useful Imaging Tool in Monitoring Prostate Tumor Growth in the Orthotopic Mouse Model

Ultrasound imaging was conducted starting from 1 week after the cell inoculation. Orthotopic prostate tumor was found to be detectable by ultrasound as early as 2 weeks after the cell inoculation, suggesting great sensitivity of ultrasound in CaP detection. Figure 1 illustrates several characteristics of the prostate and its surrounding accessory organs (*A*) as well as prostate tumor (*B*) that can be observed using 2D ultrasound imaging. Firstly, prostate tumor shows a hypoechoic ring surrounding a central region of heterogeneous texture. The appearance of a hypoechoic outer ring appears to be an important factor that allows prostate tumors to be detected in ultrasound images. Secondly, the male urinary and reproductive accessory organs such as bladder and seminal vesicles are recognizable

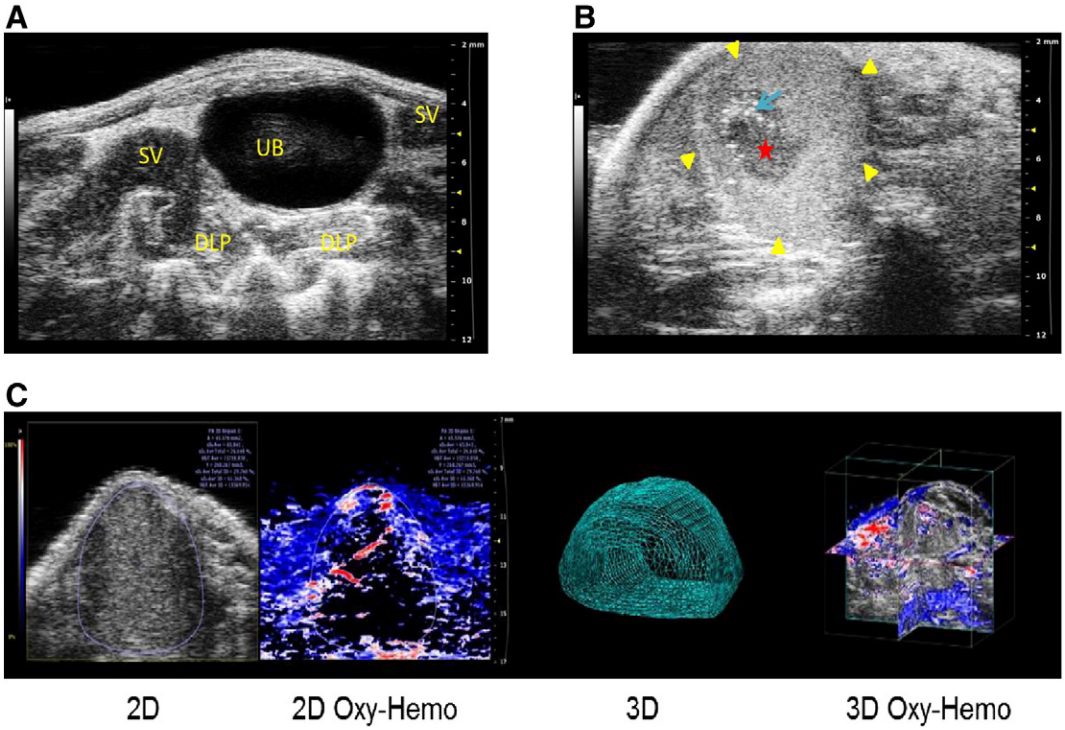

Figure 1. Representative 2D ultrasound images of prostate and prostate tumor. Prostate parts and its surrounding accessory organs (A), and prostate tumor (B) can be observed using 2D ultrasound imaging. Prostate tumor was delineated with yellow triangles; the red star (hypoechoic area) indicates hemorrhage; the blue arrow (hyperechoic area) indicates calcification formed within the tumor. Photoacoustic images were taken 3 weeks post cell inoculation. In Oxy-Hemo mode, blue indicates 0% O_2 saturation, whereas red indicates 100% O_2 saturation (C). *Avr*, average; *DLP*, dorsolateral prostate; *HbT*, hemoglobin concentration; *SV*, seminal vesicle; *UB*, urinary bladder.

in the ultrasound images, facilitating the identification of CaP. Finally, it was found that normal prostate is brighter than surrounding healthy tissues in the ultrasound images, so normal prostate tissue is unlikely to be misclassified as cancerous by ultrasound imaging.

PA Ultrasound Imaging As a Useful Tool in Monitoring Microenvironmental Changes in the CaP Orthotopic Mouse Model

Figure 1*C* shows PA functional maps superimposed on 2D B-mode images including area of ROI, average sO_2, and average hemoglobin concentration of ROI as well as tumor volume, tumor average sO_2, and tumor average after 3D rendering. It also enables display of blood oxygenation surrounding the tumor and tumor vasculature and angiogenesis.

Longitudinal Imaging of Tumor Progression

Figure 2, *A–E* shows the representative 2D images from 3D scans of four different time points in a mouse that developed a large ventral prostate tumor. The tumor was first detected 2 weeks post cell inoculation, designated week 0. Figure 2*A* shows a 2D ultrasound image obtained at week 0. Figure 2, *B–E* shows the images of the same tumor on week 1, 2, 3, and 4, respectively. 3D scans were loaded into the analysis software and reconstructed, and then the tumor was manually outlined. Figure 2, *F–J* depicts representative images of 3D rendering of CaP from the same mouse at different time points of week 0, 1, 2, 3, and 4. Figure 2*K* presents the gross pathology tumor specimen that was harvested on week 5. The hematoxylin and eosin slide demonstrates an extensive, poorly differentiated high-grade CaP xenograft tissue (Figure 2*L*). Longitudinal tumor volume measurements were obtained from all eight mice. The representative tumor volumes from three mice were plotted against time in Figure 3*A*. The results indicate that the exponential growth functions fit the volume data well (r^2 = 0.948, 0.955, and 0.953 for mouse 1, 2, and, 3, respectively).

Agreement of Ultrasound Imaging and Gross Pathology Volume Measurements

Paired volume measurements obtained from 3D ultrasound images and gross pathology specimens harvested at the end of experiment from eight mice are plotted in Figure 3*B*. The plot shows a straight-line fit to the data obtained by linear regression. Pearson's correlation coefficient is r = 0.95, indicating a significant ($P < .001$) correlation between the ultrasound and gross pathology measurement. The Bland-Altman scatter plot (Figure 3*C*) shows the close agreement between ultrasound and gross pathology at the end of the experiment. The difference was plotted against the average, and the SD of the difference (bias) was 11.6 mm^3, which was small compared with the true volume of the tumors.

Discussion

The development of imaging equipment and reporter probes has improved researchers' ability to study mouse models of CaP, such as the orthotopic model. These technologies can now be used to continuously monitor *in vivo* tumor development, providing data that traditionally used to be unavailable premortem, such as tumor volume and growth curves. Ideally, a small-animal cancer imaging technology should be sensitive to tumors; produce high-quality

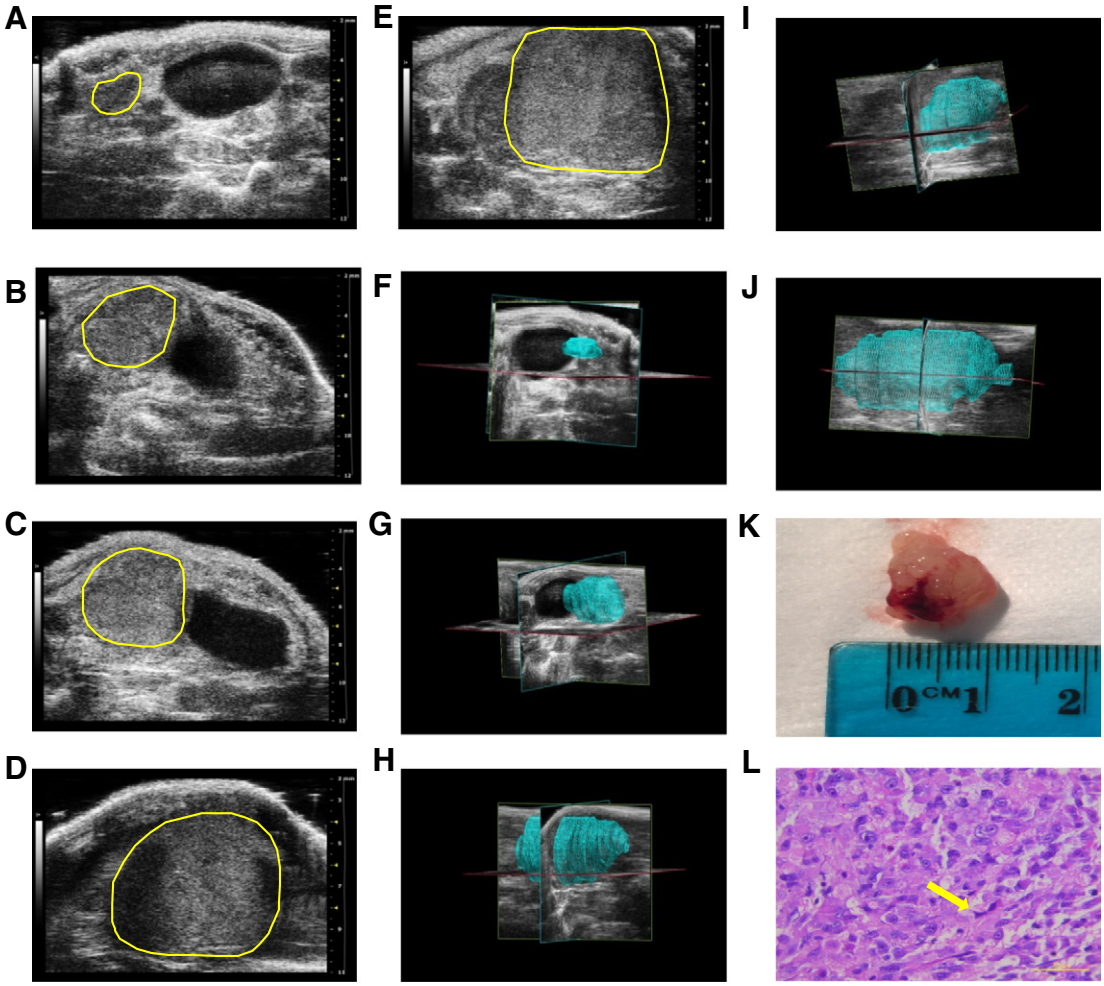

Figure 2. Longitudinal 2D and 3D ultrasound images of prostate tumors with gross pathology and histopathology. (A–E) Transverse prostate tumor (outlined by yellow line) obtained from the same mouse on five different time points (week 0-4). (F–J) 3D reconstructed prostate tumor (outlined by blue wire) acquired from the same mouse on five different time points (week 0-4). (K) Gross specimen of the same tumor harvested at the end of the experiment. (L) Hematoxylin and eosin slide from the same specimen shows a high-grade, poorly differentiated (yellow arrow) CaP of the same tumor (magnification, ×400).

images; acquire images rapidly; and employ equipment that is inexpensive to purchase, feasible to operate, and easy to maintain. Furthermore, when frequent longitudinal studies are required, the imaging examination should be harmless and noninvasive to the animal so that as many imaging sessions can be done as necessary without imposing the risk to the animals.

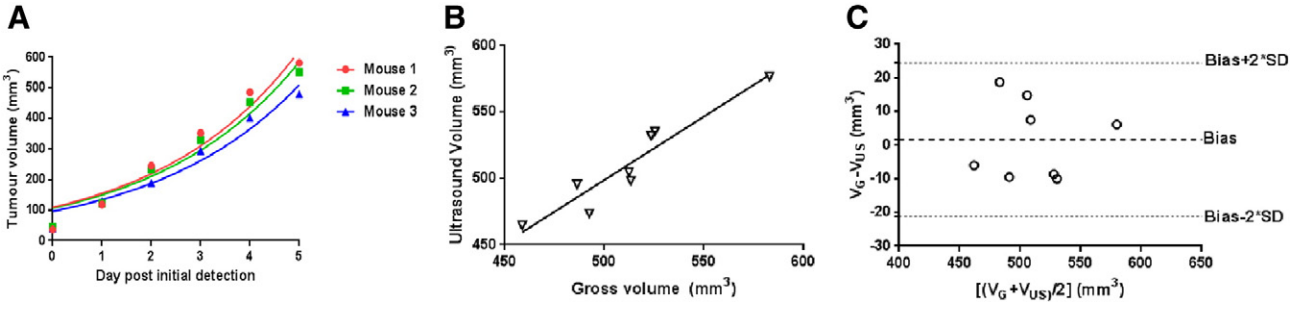

Figure 3. Exponential growth curves for longitudinal tumor volume measurements and agreement of 3D ultrasound imaging and gross pathology volume measurements. (A) Prostate tumor volumes from three representative mice were plotted against time, with fitted exponential growth curves, $r^2 = 0.948$, 0.955, and 0.953 for mouse 1, 2, and 3, respectively. (B) Good correlation of eight paired tumor volumes measured by 3D ultrasound imaging and gross pathology was demonstrated by linear regression (Pearson's $r = 0.95$, $P < .001$). (C) Bland-Altman analysis of agreement of eight paired tumor volume measurements by 3D ultrasound imaging and gross pathology was plotted.

Ultrasound imaging provides an attractive combination of the characteristics required for a small-animal imaging technology mentioned above. Ultrasound is nonionizing, is noninvasive, and provides a good soft-tissue contrast without the need of injection of imaging developing agents. In animals, it has been used to monitor interventional procedures such as *in utero* transgene or cell implantations [12], and tumor development of various kinds of cancers including breast cancer [13], hepatocarcinoma [14], ovarian cancer [15], and CaP [16]. The system used in this study permits a rapid survey of mouse CaP, thereby improving the efficiency of multiple-animal longitudinal studies.

In this study, we used 2D and 3D ultrasound imaging to monitor the tumor growth in an orthotopic tumor xenograft model and compared the acquired data to the true tumor volume. Our results indicate that ultrasound imaging, whether in 2D or 3D mode, is able to clearly detect CaP in the orthotopic mouse model. Our current findings also showed a good correlation and agreement of tumor volumes measured by 3D ultrasound imaging and gross pathology. In addition, this study also demonstrated that repeated imaging sessions had been well tolerated by the mice, suggesting that 3D ultrasound imaging is an ideal technique to monitor longitudinal tumor growth in the orthotopic CaP mouse model. Furthermore, we also found that the latest development of PA imaging is well suited to small-animal imaging. Because it is a lately developed technology, not many investigations have been done regarding this methodology. The characteristics of PA can be used in the tumor microenvironment studies, such as hypoxia, angiogenesis, and tumor response to cancer therapies.

Challenges of ultrasound imaging include smaller penetration depth, inability to image air-filled organs, vulnerability of ultrasound of easily being scattered, and operator-subjective image variability. Also, it does not produce whole-body cross-sectional images as computed tomography and magnetic resonance imaging (MRI) do. Moreover, it is hard to use ultrasound to detect CaP tumorigenesis in an early stage (1 week post cell inoculation) as well as potential metastasis, whereas MRI was able to provide cross-sectional images of a prostate tumor as early as 1 week and any suspect metastasis could easily be distinguished. Lastly, the tumor volume measurement in 3D imaging is largely dependent on an operator. MRI is a versatile imaging tool with high soft-tissue contrast and can be used to obtain anatomical, physiological, and molecular information about tumors. Our group used T2-fluid attenuation inversion recovery (FLAIR) MRI sequence to monitor the tumor growth in an orthotopic CaP model in NODSCID mice. We found that CaP tumorigenesis could be detected as early as 1 week post cell inoculation and tumor is better delineated from surrounding anatomies (unpublished data). High-resolution MRI is by far one of the most useful imaging tools to visualize tumors size, location, metastatic burden, and phenotype. Investigations on comparison of ultrasound and MRI in monitoring tumor growth, as well as on using MRI to monitor longitudinal tumor growth, are ongoing in our group.

This study demonstrates that ultrasound is a feasible, economical, and sensitive method to monitor longitudinal tumor growth in an orthotopic CaP mouse model. Future investigations should be directed to improve the image quality and field of view, automate the tumor volume measurement to address the current challenges, and optimize PA imaging operation and develop other new molecular imaging technologies using ultrasound to supplement existing modalities.

Acknowledgements

This study was supported by NHMRC Career Development Fellowship, Surgical & Urological Research Foundation, Cancer Research Trust Fund at Cancer Care Centre, and Prostate and Breast Cancer Foundation. We thank Julia Beretov from Anatomical Pathology, SEALS, St George Hospital, for technical support in histopathology. We also thank Carl Power from Biological Resource Imaging Laboratory, University of New South Wales, for technical support in animal model establishment and imaging.

References

[1] Siegel R, Ma J, Zou Z, and Jemal A (2014). Cancer statistics, 2014. *CA Cancer J Clin* **64**, 9–29.

[2] Therasse P, Arbuck SG, Eisenhauer EA, Wanders J, Kaplan RS, Rubinstein L, Verweij J, Van Glabbeke M, van Oosterom AT, and Christian MC, et al (2000). New guidelines to evaluate the response to treatment in solid tumors. European Organization for Research and Treatment of Cancer, National Cancer Institute of the United States, National Cancer Institute of Canada. *J Natl Cancer Inst* **92**, 205–216.

[3] Weissleder R (2002). Scaling down imaging: molecular mapping of cancer in mice. *Nat Rev Cancer* **2**, 11–18.

[4] Turnbull DH, Ramsay JA, Shivji GS, Bloomfield TS, From L, Sauder DN, and Foster FS (1996). Ultrasound backscatter microscope analysis of mouse melanoma progression. *Ultrasound Med Biol* **22**, 845–853.

[5] Wang X, Pang Y, Ku G, Xie X, Stoica G, and Wang LV (2003). Noninvasive laser-induced photoacoustic tomography for structural and functional in vivo imaging of the brain. *Nat Biotechnol* **21**, 803–806.

[6] Kruger RA (1994). Photoacoustic ultrasound. *Med Phys* **21**, 127–131.

[7] Laufer J, Delpy D, Elwell C, and Beard P (2007). Quantitative spatially resolved measurement of tissue chromophore concentrations using photoacoustic spectroscopy: application to the measurement of blood oxygenation and haemoglobin concentration. *Phys Med Biol* **52**, 141–168.

[8] Siphanto RI, Thumma KK, Kolkman RG, van Leeuwen TG, de Mul FF, van Neck JW, van Adrichem LN, and Steenbergen W (2005). Serial noninvasive photoacoustic imaging of neovascularization in tumor angiogenesis. *Opt Express* **13**, 89–95.

[9] Li Y, Song E, Abbas Rizvi SM, Power CA, Beretov J, Raja C, Cozzi PJ, Morgenstern A, Apostolidis C, and Allen BJ, et al (2009). Inhibition of micrometastatic prostate cancer cell spread in animal models by 213Bilabeled multiple targeted alpha radioimmunoconjugates, [Research Support, Non-U.S. Gov't]. *Clin Cancer Res* **15**, 865–875.

[10] Hao J, Madigan M C, Khatri A, Power C A, Hung T T, Beretov J, Chang L, Xiao W, Cozzi PJ, and Graham PH, et al (2012). In vitro and in vivo prostate cancer metastasis and chemoresistance can be modulated by expression of either CD44 or CD147, [Research Support, Non-U.S. Gov't]. *PLoS One* **7**, e40716.

[11] Bland JM and Altman DG (1986). Statistical methods for assessing agreement between two methods of clinical measurement. *Lancet* **1**, 307–310.

[12] Liu A, Joyner AL, and Turnbull DH (1998). Alteration of limb and brain patterning in early mouse embryos by ultrasound-guided injection of Shh-expressing cells. *Mech Dev* **75**, 107–115.

[13] Han HD, Jeon YW, Kwon HJ, Jeon HN, Byeon Y, Lee CO, Cho SH, and Shin BC (2015). Therapeutic efficacy of doxorubicin delivery by a CO generating liposomal platform in breast carcinoma. *Acta Biomater* **24**, 279–285.

[14] Choi BI, Lee JM, Kim TK, Burgio MD, and Vilgrain V (2015). Diagnosing borderline hepatic nodules in hepatocarcinogenesis: imaging performance. *AJR Am J Roentgenol* **205**, 10–21.

[15] Prada F, Del Bene M, Moiraghi A, Casali C, Legnani FG, Saladino A, Perin A, Vetrano IG, Mattei L, and Richetta C, et al (2015). From grey scale B-Mode to elastosonography: multimodal ultrasound imaging in meningioma surgery—pictorial essay and literature review. *BioMed Res Int* **2015**, 925729.

[16] Wirtzfeld LA, Wu G, Bygrave M, Yamasaki Y, Sakai H, Moussa M, Izawa JI, Downey DB, Greenberg NM, and Fenster A, et al (2005). A new three-dimensional ultrasound microimaging technology for preclinical studies using a transgenic prostate cancer mouse model. *Cancer Res* **65**, 6337–6345.